Adenovirus-mediated overexpression of sphingomyelin synthases 1 and 2 increases the atherogenic potential in mice

Jibin Dong,[1,*] Jin Liu[1,†] Bin Lou,[*] Zhiqiang Li,[†] Xun Ye,[§] Manping Wu,[2,*] and Xian-Cheng Jiang[2,†]

School of Pharmacy,* Fudan University, Shanghai, People's Republic of China; Department of Anatomy and Cell Biology,† State University of New York Downstate Medical Center, Brooklyn, NY; and Department of Pharmacology,§ College of Basic Medical Sciences, Shanghai Jiaotong University, Shanghai, People's Republic of China

Abstract **Sphingomyelin synthase 1 (SMS1) and SMS2 are two isoforms of SMS, the last enzyme for sphingomyelin (SM) biosynthesis. To evaluate the role of SMS in vivo in terms of plasma lipoprotein metabolism, we generated recombinant adenovirus vectors containing human SMS1 cDNA (AdV-SMS1), SMS2 cDNA (AdV-SMS2), or the reporter LacZ cDNA (AdV-LacZ) as a control. On day 7 after intravenous infusion of 2×10^{11} particles of both AdV-SMS1 and AdV-SMS2 into mice, liver SMS1 and SMS2 mRNA levels as well as SMS activity were significantly increased (2.5-, 2.7-, 2.1-, and 2.3-fold, respectively; $P < 0.001$). Lipoprotein analysis indicated that AdV-SMS1 and AdV-SMS2 treatment caused no changes of total SM and cholesterol levels but significantly decreased HDL-SM and HDL-cholesterol (42% and 38%, and 27% and 25%, respectively; $P < 0.05$). It also significantly increased non-HDL-SM and non-HDL-cholesterol levels (50% and 35%, and 64% and 61%, respectively; $P < 0.05$) compared with AdV-LacZ controls. SDS–PAGE showed a significant increase in apolipoprotein B (apoB; $P < 0.01$) but no changes in apoA-I levels. Moreover, we found that non-HDL from both AdV-SMS1- and AdV-SMS2-treated mice was significantly aggregated after treatment with a mammalian sphingomyelinase, whereas lipoproteins from control animals did not aggregate. To investigate the mechanism of HDL changes, we measured liver scavenger receptor class B type I (SR-BI) levels by Western blot. We found that AdV-SMS1 and AdV-SMS2 mouse liver homogenates contained 50% and 55% higher SR-BI levels than in controls, whereas no change was observed in hepatic ABCA1 levels. An HDL turnover study revealed an increase of plasma clearance rates for [^{3}H]cholesteryl oleyl ether-HDL but not for [^{125}I]HDL in both AdV-SMS1 and AdV-SMS2 mice compared with controls. In conclusion, adenovirus-mediated SMS1 and SMS2 overexpression increased lipoprotein atherogenic potential. Such an effect may contribute to the increased plasma SM levels observed in animal models of atherosclerosis and in human patients with coronary artery disease.**—Dong, J., J. Liu, B. Lou, Z. Li, X. Ye, M. Wu, and X-C. Jiang. **Adenovirus-mediated overexpression of sphingomyelin synthases 1 and 2 increases the atherogenic potential in mice.** ***J. Lipid Res.*** **2006.** 47: **1307–1314.**

Supplementary key words lipoprotein • atherosclerosis • sphingolipid

Sphingomyelin (SM) is one of the major phospholipids in the circulation (1). It has been known for some time that plasma SM is an independent risk factor for coronary heart disease (2) and that it accumulates in atheromas both in humans and in animal models (3, 4). LDL extracted from human atherosclerotic lesions is much richer in SM than LDL from plasma (5, 6). Plasma SM levels in apolipoprotein E (apoE) knockout mice are 4-fold higher than those in wild-type mice (7), and this may partly explain the increased atherosclerosis in these animals (8). SM levels are increased 5-fold in VLDL from hypercholesterolemic rabbits (9). We and others recently demonstrated for the first time that intraperitoneal myriocin (an SM de novo synthesis inhibitor) administered to apoE knockout mice dramatically decreased SM in the plasma and significantly decreased areas of atherosclerotic lesion (10, 11). These data suggest that plasma SM may play a promoting role in the development of atherosclerosis.

Significant evidence has been presented to confirm the existence of lipid rafts in membranes enriched with sphingolipids and cholesterol in the liquid-ordered phase (12, 13). SM is a major component of sphingolipids. Lipid raft domains have recently drawn extensive attention because they may play important roles as platforms for the functioning of many receptors and for signal transduction in these membranes (14–17). Therefore, changes of SM bio-

Manuscript received 25 January 2006 and in revised form 21 February 2006.

Published, JLR Papers in Press, February 28, 2006.
DOI 10.1194/jlr.M600040-JLR200

[1] J. Dong and J. Liu contributed equally to this report.
[2] To whom correspondence should be addressed.
e-mail: mpwu@shmu.edu.cn (M.W.);
xjiang@downstate.edu (X-C.J.)

synthesis may have an impact on receptor-mediated lipoprotein metabolism, thus influencing lipoprotein levels in the circulation. Sphingomyelin synthase (SMS) is the last enzyme involved in the SM biosynthesis that transfers the phosphorylcholine moiety from phosphatidylcholine onto the primary hydroxyl of ceramide-producing SM and diglyceride (18). Evidence from the literature supports the belief that SM can be synthesized at more than one subcellular site. Many studies indicate that SM synthase is located mainly in the *cis*-medial Golgi (19–21) and plasma membranes (22–24). In addition, SMS activity has been found in chromatin, and chromatin-associated SMS modifies SM content (25–27). Despite the biological importance of SMS, understanding of the molecular mechanisms of its regulation and its relationship with plasma SM levels is limited by the fact that no successful purification of this protein has been achieved. The gene(s) encoding for this activity was not even cloned until recently (28, 29). There are two isoforms of mammalian SMS genes, SMS1 and SMS2. The former is located in the *cis*-medial Golgi, whereas the latter is located on plasma membranes (28).

In this study, we used the adenovirus approach to overexpress both SMS1 and SMS2 in mice to investigate the relationship between SMS and SM metabolism. We found that both SMS1 and SMS2 overexpression significantly altered SM levels in lipoproteins and increased proatherogenic potential.

MATERIALS AND METHODS

Recombinant adenovirus generation and administration

A pShuttle-AdEasy system was used to create adenovirus vectors (Stratagene). We generated pShuttle.CMV-SMS1 and pShuttle.CMV-SMS2 by inserting full-length SMS1 and SMS2 cDNAs into the *Sal*I/*Not*I and *Not*I/*Eco*RV sites of pShuttle.CMV, respectively. Then, pShuttle.CMV-SMS1 and pShuttle.CMV-SMS2 were linearized by *Pme*I digestion and recombined with pAdEasy-1 in BJ5183 cells. Correct recombinants were selected and retransformed into *Escherichia coli* (DH-5α). Purified recombinant plasmids were linearized by *Pac*I restriction and transfected into HEK-293 cells to create adenoviruses. Recombinant viruses were propagated in HEK-293 cells, purified, and titered by standard methods, as described elsewhere (30).

The corresponding viruses were named AdV-SMS1 and AdV-SMS2. The E1 genes (nucleotides 342–3,534) and the E3 genes (nucleotides 28,138–30,818) were deleted in those virus vectors. Recombinant adenovirus containing the LacZ gene (i.e., AdV-LacZ) was purchased from Viraquest, Inc. To assess the contamination of E1+ replication-competent adenovirus, real-time PCR analysis was performed according to a protocol described elsewhere (31). Only virus preparations that contained less than one E1+ viral genome in 10^6 genomes were used in this study. An appropriate aliquot of the purified recombinant adenovirus containing 2×10^{11} particles was infused into the femoral vein of C57BL/6 mice on day 0 of the study. Seven days later, blood samples from the tail vein were obtained from mice fasted for 4 h. Samples were placed in precooled tubes containing EDTA (final concentration, 4 mM) and centrifuged at 2,500 *g* for 20 min at 4°C, and aliquots of plasma were stored at −70°C.

SMS1 and SMS2 mRNA measurement

Total RNA was isolated from livers with Trizol (Invitrogen). SMS1 and SMS2 mRNA levels were measured by RT-PCR. Briefly, 10 μg of total RNA was reverse-transcribed with random primers and murine leukemia virus reverse transcriptase (30°C for 10 min followed by 42°C for 120 min). They were amplified by PCR with 50 nM primers using the following cycling program: initial step of 94°C for 4 min; 31 cycles of 94°C for 30 s, 55°C for 30 s, and 72°C for 30 s; and final step of 72°C for 8 min. The PCR products were visualized by electrophoresis on 1.2% agarose gels. β-Actin RNA served as an internal control. The primers used for the analyses were SMS1 sense (5′-CAACATTGGCGTAGACAT-3′), SMS1 antisense (5′-TAGGAGGTACTCGTTCGTG-3′), SMS2 sense (5′-GATACAAGTCAATAGTGGGACG-3′), SMS2 antisense (5′-AGAAGTGACGAGGCGAAT-3′), β-actin sense (5′-GGGTCA-CCCACACTGTGCCCATCTA-3′), and β-actin antisense (5′-GCA-TTTGCGGTGGACGATGGAGG-3′). The gel was scanned with a Phosphorimager, and the intensity of each band was measured by Image-Pro Plus version 4.5 software (Media Cybernetics, Inc.).

Plasma lipid measurement

We used a kit for plasma and HDL-cholesterol measurement (Wako Pure Chemical Industries, Ltd., Osaka, Japan). We established new, high-throughput enzymatic methods to measure plasma and HDL-SM and phosphatidylcholine levels (32).

Liver lipid measurement

Liver ceramide and sphingosine-1-phosphate levels were measured as we reported previously (10, 33). Liver total SM, cholesterol, and triglyceride were quantified in lipid extracts of liver using enzymatic reagents as described previously (32, 34, 35).

Lipoprotein analysis

Lipoprotein profiles were obtained by fast-protein liquid chromatography using a Sepharose 6B column. The fraction size was 0.7 ml per fraction. Plasma lipoproteins were isolated by adjusting the density to 1.21 g/ml and then by buoyant density ultracentrifugation. Apolipoproteins were separated through a 4–20% SDS-polyacrylamide gel. Coomassie blue-stained SDS-PAGE gels were destained, and proteins were quantified using Image-Pro Plus software (Media Cybernetics, Inc.).

SMS activity assay

SMS activity was measured as described previously (36). Briefly, the liver was homogenized in a buffer containing 50 mM Tris-HCl, 1 mM EDTA, 5% sucrose, and protease inhibitors. The homogenate was centrifuged at 5,000 rpm for 10 min, and the supernatant was used for SMS activity assay. The reaction system contained 10 mM HEPES (pH 7.4), 3 mM $MnCl_2$, C6-nitrobenzoxadiazole-ceramide (60 μg/600 μl), and phosphatidylcholine (2 μg/600 μl). The mixture was incubated at 37°C for 2 h. Lipids were extracted in chloroform-methanol (2:1), dried under N_2 gas, and separated by TLC. The plate was scanned with a Phosphorimager, and the intensity of each band was measured by Image-Pro Plus version 4.5 software (Media Cybernetics, Inc.).

Atherogenic lipoprotein aggregation assay

Lipoprotein aggregation was assessed as described previously (7). In brief, LDL (4 μg of cholesteryl ester) was incubated with 25 μl of macrophage culture medium containing secretory sphingomyelinase (SMase) in 0.1 M Tris-HCl buffer, pH 7.2, at

37°C for 4 h. The turbidity of the samples was assessed by measuring the optical density at 430 nm.

Western blot for mouse liver scavenger receptor class B type I and ABCA1

SDS-PAGE was performed on a 4–20% SDS-polyacrylamide gradient gel using 200 μg (protein) of mouse liver homogenate, and the separated proteins were transferred to nitrocellulose membranes. Western blot analysis for mouse scavenger receptor class B type I (SR-BI) and ABCA1 was performed using a polyclonal anti-mouse SR-BI antibody and a polyclonal anti-mouse ABCA1 antibody (Novus Biologicals). Horseradish peroxidase-conjugated rabbit polyclonal antibody to mouse IgG (Novus Biologicals) was used as a secondary antibody. The SuperSignal West detection kit (Pierce) was used for the detection step. The maximum intensity of each band was measured by Image-Pro Plus version 4.5 software (Media Cybernetics, Inc.) and used for analysis.

In vivo turnover studies

Mouse HDL was isolated by ultracentrifugation ($1.063 < d < 1.21$ g/ml). Mice were injected intravenously with HDL that was labeled with [^{3}H]cholesteryl oleyl ether ([^{3}H]CEt) (2×10^6 cpm) or ^{125}I (1×10^6 cpm). After injection, blood (70 μl) was taken from the tail vein at 0.25, 0.5, 1, 2, 5, 9, and 24 h for determination of radioactivity. The clearance rate was calculated from the decay curves of [^{3}H]CEt and ^{125}I according to the Matthews method (37).

Statistical analysis

Differences between groups were tested by Student's *t*-test. Data are presented as means ± SD. $P < 0.05$ was considered significant.

RESULTS

To investigate the in vivo role of SMS1 and SMS2, we used AdV-SMS1 and AdV-SMS2 to express human SMS1 and SMS2 in male C57BL/6J mice. AdV-LacZ was used as a control. RT-PCR of RNA prepared from mouse liver was performed, revealing a 2.5-fold increase of SMS1 mRNA and a 2.7-fold increase of SMS2 mRNA levels in mice treated with AdV-SMS1 and AdV-SMS2, respectively, compared with AdV-LacZ-treated mice (**Fig. 1**). The liver SMS activity assay confirmed the overexpression of SMS1 and SMS2 in mouse liver. AdV-SMS1 administration caused a 2.1-fold increase in liver SMS activity, whereas AdV-SMS2 caused a 2.3-fold increase, compared with controls (**Fig. 2**).

As indicated in **Table 1**, plasma lipid analysis by precipitation (AdV-SMS1 mice vs. AdV-LacZ mice, and AdV-SMS2 mice vs. AdV-LacZ mice) showed a significant reduction in HDL-SM (42% and 38%, respectively; $P < 0.05$ and $P < 0.02$) and HDL-cholesterol (27% and 25%, respectively; $P < 0.05$ and $P < 0.02$). There was also a significant induction of non-HDL-cholesterol-SM (50% and 35%, respectively; $P < 0.01$ and $P < 0.05$) and non-HDL-cholesterol (64% and 61%, respectively; $P < 0.01$).

The distribution of lipids was likewise determined by fast-protein liquid chromatography of pooled plasma samples. This demonstrated that HDL-SM and HDL-cholesterol were significantly decreased in AdV-SMS1 and AdV-SMS2 mice compared with AdV-LacZ mice (**Fig. 3**). Assessment of the apolipoprotein composition of centrifugally isolated total lipoproteins by reducing SDS-PAGE revealed a significant increase of apoB ($P < 0.01$) but not apoA-I (**Fig. 4**).

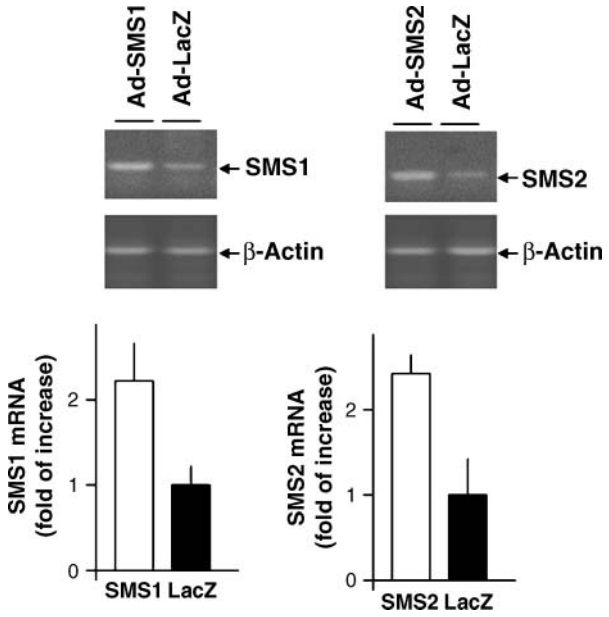

Fig. 1. Sphingomyelin synthase 1 (SMS1) and SMS2 mRNA measurement. SMS1 and SMS2 mRNA levels were measured by RT-PCR as described in Materials and Methods. β-Actin was used as an internal control. Values shown are means ± SD. Data were analyzed with Student's *t*-test (* $P < 0.001$; n = 6).

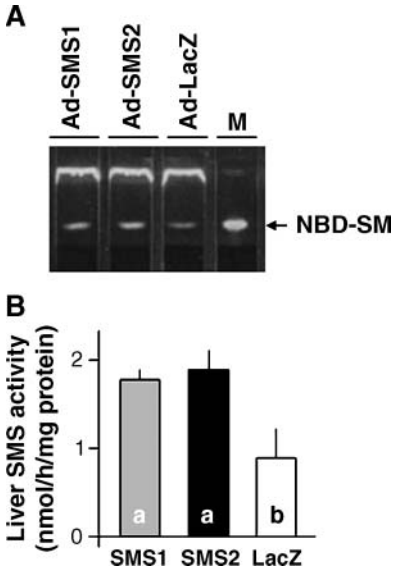

Fig. 2. SMS activity assay. The liver was homogenized. The reaction system contained liver homogenate (200 μg of protein), C6-nitrobenzoxadiazole-ceramide, and phosphatidylcholine. The mixture was incubated at 37°C for 2 h. Lipids were extracted in chloroform-methanol (2:1), dried under N_2 gas, and then separated by TLC. The fluorescence intensity of each spot was determined as described in Materials and Methods. Values shown are means ± SD. Data were analyzed with Student's *t*-test (* $P < 0.001$; n = 6). M, marker; Columns labeled with lower-case letters are statistically different by student's *t*-test, $P < 0.01$.

TABLE 1. Plasma lipid measurement in AdV-SMS1, AdV-SMS2, and AdV-LacZ (control) mice

Mouse	Cholesterol	SM	Phosphatidylcholine	HDL-Cholesterol	HDL-SM	Non-HDL-Cholesterol	Non-HDL-SM
	mg/dl						
AdV-LacZ	109 ± 19 a	43 ± 7 a	139 ± 11 a	81 ± 11 a	24 ± 5 a	28 ± 7 a	20 ± 3 a
AdV-SMS1	105 ± 21 a	44 ± 6 a	133 ± 21 a	59 ± 7 b	14 ± 3 b	46 ± 10 b	30 ± 5 b
AdV-SMS2	106 ± 18 a	42 ± 4 a	135 ± 16 a	61 ± 8 b	15 ± 6 b	45 ± 9 b	27 ± 4 b

SM, sphingomyelin; SMS, sphingomyelin synthase. Values shown are means ± SD (n = 6). Columns labeled with different lowercase letters are statistically different ($P < 0.05$).

We next sought to determine whether enrichment of SM in non-HDL would contribute to the atherogenicity of these particles. As stated above, there is evidence to suggest that hydrolysis of lipoprotein SM by an arterial wall SMase may lead to lipoprotein aggregation (38). Therefore, we reasoned that enrichment of lipoproteins with SM might increase their susceptibility to SMase-induced aggregation by increasing substrate availability to the enzyme (7). To test this hypothesis, we used SMase, which is secreted by J774 macrophages. As shown in **Fig. 5**, non-HDL from AdV-SMS1- and AdV-SMS2-injected mice was significantly aggregated after treatment with SMase, whereas these lipoproteins from AdV-LacZ-administered mice did not aggregate. We also measured plasma SMase activity by the method described previously (39), finding no significant changes between AdV-LacZ and AdV-SMS1 or AdV-SMS2 treatment (data not shown). This suggested that secreted SMase activity does not contribute to the enrichment of SM in non-HDL.

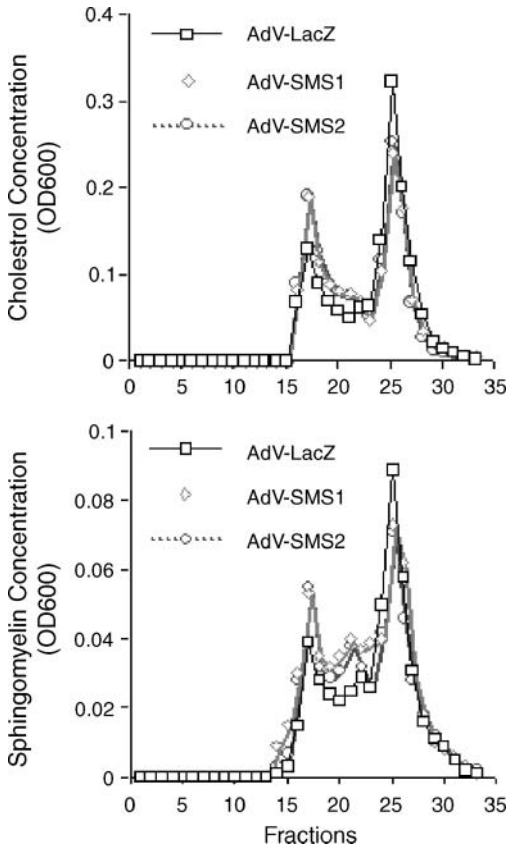

Fig. 3. Mouse plasma lipoprotein analysis by fast-protein liquid chromatography. A 200 μl aliquot of pooled plasma (from six animals) was loaded onto a Sepharose 6B column and eluted with 50 mM Tris and 0.15 M NaCl (pH 7.5). An aliquot of each fraction was used for the determination of cholesterol and sphingomyelin. OD600, optical density at 600 nm.

We also measured hepatic SM, cholesterol, and triglyceride as well as ceramide and sphingosine-1-phosphate levels. We did not observe significant changes of these lipids, although there was an increasing tendency for SM levels ($P = 0.07$) (**Tables 2, 3**). This result suggests that both AdV-SMS1 and AdV-SMS2 might cause SM distribution but not total mass changes in the liver.

SR-BI is an HDL receptor that plays an essential role in the hepatic uptake of plasma HDL-derived lipid into the liver (40, 41). Because the adenovirus gene delivery system mainly mediates liver overexpression, the observed reduction of HDL-SM and HDL-cholesterol (Table 1) in AdV-SMS1 and AdV-SMS2 mice may reflect the alteration of SR-BI expression levels. We next determined SR-BI levels by Western blot, finding that AdV-SMS1 and AdV-SMS2 mouse liver has significantly higher SR-BI levels than control liver (75% and 78%, respectively; $P < 0.01$) (**Fig. 6**). This suggests that both mice have a stronger capacity to take up HDL-lipid selectively than do the controls. We also measured ABCA1, an HDL generator (42), by Western blot analysis, finding no significant alterations (data not shown).

To further evaluate the consequences of a defect in SR-BI expression, we carried out HDL turnover studies in AdV-SMS1, AdV-SMS2, and control mice using [^{3}H]CEt- and ^{125}I-labeled mouse HDL. Mice were injected with double-labeled HDL intravenously (femoral vein). The plasma clearance rates of [^{3}H]CEt-HDL in AdV-SMS1 and AdV-SMS2 mice were 40% and 44% higher than those in controls, respectively ($P < 0.02$) (**Table 4**), whereas the clearance rates of ^{125}I-HDL did not change, indicating a defect of cholesteryl ester selective uptake.

DISCUSSION

In this study, we have demonstrated for the first time that adenovirus-mediated SMS1 and SMS2 expression causes significant *1*) increases of hepatic SMS1 and SMS2 mRNA levels; *2*) increases of hepatic SMS activity; *3*) increases of plasma non-HDL-SM and non-HDL-cholesterol levels; *4*) increases of non-HDL particle aggregation after mammalian SMase treatment; *5*) increases of liver SR-BI protein levels and cholesteryl ester selective uptake; and *6*) decreases of plasma HDL-SM and HDL-cholesterol levels.

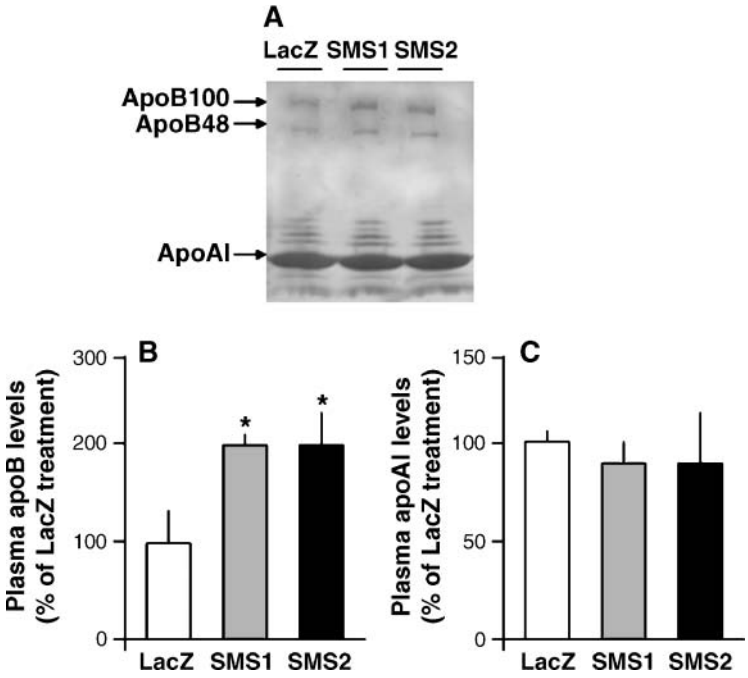

Fig. 4. SDS-PAGE analysis of apolipoproteins. Plasma lipoproteins (d < 1.21 g/ml) were separated by preparative ultracentrifugation as described (22). SDS-PAGE was performed on 4–20% SDS-polyacrylamide gradient gels, and the apolipoproteins were stained by Coomassie brilliant blue and scanned as described (22). Values shown are means ± SD. Data were analyzed with Student's *t*-test (* $P < 0.01$; n = 4). ApoB, apolipoprotein B.

SM is a ubiquitous structural component of mammalian cell membranes and lipoproteins, and its cellular and plasma levels are regulated by both synthetic and catabolic pathways. In particular, the biochemical synthesis of SM occurs through the action of a serine palmitoyl-CoA transferase (SPT; the first enzyme of SM biosynthesis), 3-ketosphinganine reductase, ceramide synthase, dihydroceramide desaturase, and SMS (the last enzyme of SM biosynthesis). Many reports have demonstrated that SPT is the key enzyme for all sphingolipid biosynthesis (10). Pharmacologic inhibition of SPT significantly decreases plasma SM levels, thus decreasing atherosclerosis in mouse models (10, 11).

There is some evidence that SMS is also a key factor in SM biosynthesis. Cells treated with D609, a specific SMS inhibitor, significantly decreased cellular SMS activity, which in turn significantly decreased intracellular levels of SM (38) as well as SM in the cell culture medium (Z. Li and X-C. Jiang, unpublished observation). Moreover, SMS activity can be regulated. It has been shown that 25-hydroxycholesterol stimulates SMS in Chinese hamster ovary cells (43, 44). It has also been demonstrated that the activity of SMS is enhanced under conditions of increased proliferation, such as in regenerating rat liver (45), SV-40 transformation of human fibroblasts (46), and highly malignant hepatoma (47). Additionally, it is known that SMS activity is inhibited by tumor necrosis factor-α in Kym-1 rhabdomyosarcoma cells before the onset of tumor necrosis factor-α-induced apoptosis and that this inhibition is a caspase-dependent event (48). In this study, we have demonstrated that overexpressing both SMS1 and SMS2 in mouse liver causes significant changes of SM and cholesterol in circulating HDL and non-HDL. This suggests that manipulating both SMS1 and SMS2 activity might have an important impact on the development of atherosclerosis.

It is well known that a decrease of HDL-cholesterol is closely related to atherogenesis (49). HDL levels are

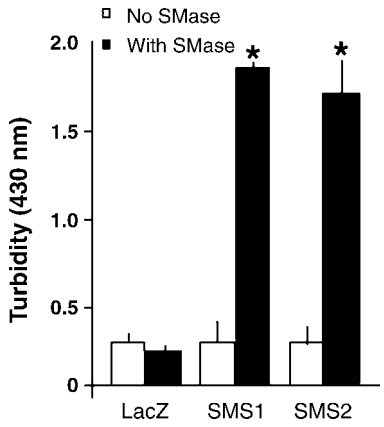

Fig. 5. In vitro aggregation of atherogenic lipoproteins induced by macrophage-derived secreted-sphingomyelinase. Non-HDL particles (d < 1.063 g/ml) were isolated from AdV-SMS1-, AdV-SMS2-, and AdV-LacZ-treated mouse plasma. Four micrograms (by cholesteryl ester mass) of non-HDL was incubated with 25 μl of macrophage culture medium containing SMase in 0.1 M Tris-HCl buffer, pH 7.2, at 37°C for 4 h. The turbidity of the samples was evaluated by measurement of optical density at 430 nm. Values shown are means ± SD. Data were analyzed with Student's *t*-test (* $P < 0.0001$; n = 4).

TABLE 2. Hepatic lipid concentrations in AdV-SMS1, AdV-SMS2, and AdV-LacZ mice

Mouse	SM	Cholesterol	Triglyceride
	mg/g liver		
AdV-LacZ	0.9 ± 0.2	5.2 ± 0.6	15.3 ± 2.1
AdV-SMS1	1.2 ± 0.4	5.5 ± 1.2	16.1 ± 1.9
AdV-SMS2	1.3 ± 0.3	5.6 ± 0.9	16.2 ± 3.3

Values shown are means ± SD (n = 4).

TABLE 3. Liver sphingolipid measurement in AdV-SMS1, AdV-SMS2, and AdV-LacZ mice

Mouse	C18:1Cer	C14Cer	C16Cer	C18Cer	C20Cer	C24Cer	C24:1Cer	S1P
	nM							
AdV-LacZ	2 ± 1	9 ± 2	8 ± 3	17 ± 2	30 ± 5	639 ± 78	959 ± 199	131 ± 13
AdV-SMS1	2 ± 1	9 ± 1	10 ± 4	16 ± 6	33 ± 4	702 ± 66	987 ± 167	130 ± 11
AdV-SMS2	3 ± 1	9 ± 2	8 ± 2	15 ± 3	32 ± 9	669 ± 59	931 ± 221	138 ± 28

Cer, ceramide; S1P, sphingosine-1-phosphate. Values shown are means ± SD (n = 3 animals tested).

regulated not only by factors in the circulation but also by factors located in cell membranes, including SR-BI, an HDL receptor (40, 41), and ABCA1, an HDL generator (42). In this study, we have shown that AdV-SMS1 or AdV-SMS2 administration significantly increases hepatic SR-BI (Fig. 6) but not ABCA1 expression. This effect may be directly related to the decrease of plasma HDL-SM and HDL-cholesterol levels (Table 1).

Increased SM content in non-HDL particles may be relevant to atherogenesis. The VLDL of hypercholesterolemic rabbits on an atherogenic diet shows an enrichment of SM (9). Non-HDL from apoE knockout mice is also enriched with SM (7). Accumulation of SM in atherosclerotic lesions can reach 75% of total phospholipid content (50). Lesional LDL is markedly enriched in SM, which could be an important factor in enhancing its reactivity with SMase (38). In this study, we found that after treatment with macrophage-derived SMase, non-HDL particles from AdV-SMS1- and AdV-SMS2-treated mice were markedly aggregated (Fig. 5). This property seemed to reflect increased SM content, because non-HDL from AdV-LacZ-injected mice did not show similar aggregation.

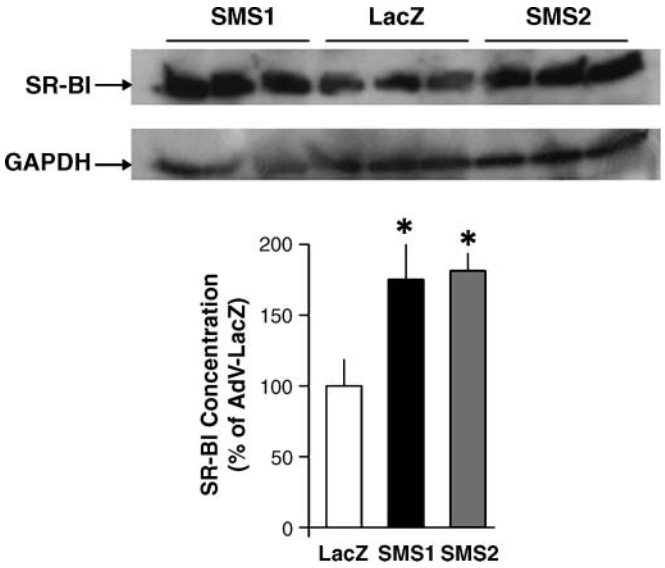

Fig. 6. Western blot analysis for scavenger receptor class B type I (SR-BI). SDS-PAGE was performed on a 4–20% SDS-polyacrylamide gradient gel using 200 μg (protein) of mouse liver homogenates, and the separated proteins were transferred to nitrocellulose membranes. Western blot analysis for mouse apolipoprotein E was performed as described in Materials and Methods. Values shown are means ± SD. Data were analyzed with Student's *t*-test (* $P < 0.01$; n = 6).

To our surprise, adenovirus-mediated SMS1 and SMS2 expression does not significantly change lipids, including SM and cholesterol, in mouse liver. There are two possible reasons for this: *1*) because adenovirus-mediated gene expression is short-lasting, we might not see the changes of lipid levels at day 7, when we euthanized the animals; and *2*) AdV-SMS1 and AdV-SMS2 might change the distribution of SM inside the hepatocytes (for instance, SM on endoplasmic reticulum, Golgi complex, and plasma membranes) but might not change the total mass. Our future studies using transgenic approaches (long-lasting) will elucidate those possibilities.

The interaction of SM and cholesterol drives the formation of plasma membrane rafts (12, 13). A general consensus has developed during the last few years that these membrane rafts represent signaling microdomains (14–17). Adenovirus-mediated SMS1 and SMS2 expression might alter the lipid raft structure. The most direct evidence in this study is the upregulation of SR-BI (Fig. 6), which is closely associated with lipid rafts on plasma membranes (51–53). SR-BI can mediate the selective uptake of cholesteryl esters from both LDL and HDL particles, but these processes are affected differently by the integrity of lipid rafts on hepatocyte membranes (51). This effect might explain why there is a reduction of HDL-cholesterol and an induction of non-HDL-cholesterol (Table 1, Fig. 3). Moreover, the HDL turnover study clearly indicated that adenovirus-mediated SMS expression diminishes cholesteryl ester selective uptake (Table 4). This result might also explain why there is no change of apoA-I levels in the circulation (Fig. 4). Furthermore, we have some promising evidence that both SMS1 and SMS2 gene knockdown affect cell plasma membrane microdomains (T. K. Hailemariam and X-C. Jiang, unpublished observation).

TABLE 4. Plasma fractional catabolic rates for ^{125}I-labeled and [^{3}H]CEt-labeled HDL in mice in AdV-SMS1, AdV-SMS2, and AdV-LacZ (control) mice

Labeling	AdV-LacZ	AdV-SMS1	AdV-SMS2
[^{3}H]CEt-HDL (pools/h)	0.092 ± 0.017	0.129 ± 0.025[a]	0.132 ± 0.019[a]
^{125}I-HDL (pools/h)	0.070 ± 0.016	0.075 ± 0.021	0.073 ± 0.015

CEt, cholesteryl oleyl ether. AdV-SMS1, AdV-SMS2, and AdV-LacZ mice were injected intravenously (femoral vein) with mouse HDL labeled with ^{125}I and [^{3}H]CEt. Blood was collected periodically from mice over 24 h after injection of labeled HDL. The fractional catabolic rates for protein and lipid were calculated from the decay of ^{125}I and [^{3}H]CEt radioactivity in whole plasma according to the Matthews method (37). Values shown are means ± SD (n = 4 mice per group).

[a] $P < 0.02$ as determined by Student's *t*-test.

Although ABCA1 is also located on plasma membranes, we found no changes of ABCA1 expression levels in AdV-SMS1- and AdV-SMS2-treated mice. There is a report indicating that cholesterol- and SM-rich membrane rafts do not provide lipid for efflux promoted by apolipoproteins through the ABCA1-mediated lipid secretory pathway and that ABCA1 is not associated with these domains (54).

Important biological roles have been clearly established for ceramide and diglyceride (substrate and product of SMS) in the regulation of fundamental cellular functions such as proliferation and apoptosis (55–58). Therefore, it has been hypothesized that SMS goes beyond the production of SM. SMS could in fact represent a key mechanism in controlling cellular levels of ceramide and diglyceride and therefore would influence functions mediated by these bioactive lipids. However, we did not observe significant changes of liver ceramide levels (Table 3). The influence of SMS1 and SMS2 overexpression on ceramide and diglyceride will be further elucidated in our future transgenic studies.

In summary, adenovirus-mediated SMS1 and SMS2 overexpression in mice creates a proatherogenic potential. Such an effect might contribute to the increased plasma SM levels observed in animal models (7, 9) of atherosclerosis as well as in human coronary artery disease (2, 59).

This work was supported by National Institutes of Health Grant HL-64735.

REFERENCES

1. Phillips, G. B., and J. T. Dodge. 1967. Composition of phospholipids and of phospholipid fatty acids of human plasma. *J. Lipid Res.* **8:** 676–681.
2. Jiang, X. C., F. Paultre, T. A. Pearson, R. G. Reed, C. K. Francis, M. Lin, L. Berglund, and A. R. Tall. 2000. Plasma sphingomyelin level as a risk factor for coronary artery disease. *Arterioscler. Thromb. Vasc. Biol.* **20:** 2614–2618.
3. Smith, E. B. 1960. Intimal and medial lipids in human aorta. *Lancet.* **1:** 799–803.
4. Kummerow, F. A., L. S. Cook, E. Wasowicz, and H. Jelen. 2001. Changes in the phospholipid composition of the arterial cell can result in severe atherosclerotic lesions. *J. Nutr. Biochem.* **12:** 602–607.
5. Hoff, H. F., and R. E. Morton. 1985. Lipoproteins containing apoB extracted from human aortas: structure and function. *Ann. N. Y. Acad. Sci.* **545:** 183–194.
6. Guyton, J. R., and K. F. Klemp. 1996. Development of the lipid-rich core in human atherosclerosis. *J. Lipid Res.* **16:** 4–11.
7. Jeong, T-s., S. L. Schissel, I. Tabas, H. J. Pownall, A. R. Tall, and X. C. Jiang. 1998. Increased sphingomyelin content of plasma lipoproteins in apolipoprotein E knockout mice reflects combined production and catabolic defects and enhances reactivity with mammalian sphingomyelinase. *J. Clin. Invest.* **101:** 905–912.
8. Plump, A. S., and J. L. Breslow. 1995. Apolipoprotein E and the apolipoprotein E-deficient mouse. *Annu. Rev. Nutr.* **15:** 495–518.
9. Rodriguez, A. L., G. C. Ghiselli, D. Torreggiani, and C. D. Sirtori. 1976. Very low density lipoproteins in normal and cholesterol-fed rabbits: lipid and protein composition and metabolism. *Atherosclerosis.* **23:** 73–83.
10. Hojjati, M. R., Z. Li, H. Zhou, S. Tang, C. Huan, E. Ooi, S. Lu, and X. C. Jiang. 2005. Effect of myriocin on plasma sphingolipid metabolism and atherosclerosis in apoE-deficient mice. *J. Biol. Chem.* **280:** 10284–10289.
11. Park, T. S., R. L. Panek, S. B. Mueller, J. C. Hanselman, W. S. Rosebury, A. W. Robertson, E. K. Kindt, R. Homan, S. K. Karathanasis, and M. D. Rekhter. 2004. Inhibition of sphingomyelin synthesis reduces atherogenesis in apolipoprotein E-knockout mice. *Circulation.* **110:** 3465–3471.
12. Simons, K., and E. Ikonen. 1997. Functional rafts in cell membranes. *Nature.* **387:** 569–572.
13. Simons, K., and G. van Meer. 1988. Lipid sorting in epithelial cells. *Biochemistry.* **27:** 6197–6202.
14. Brown, D. A., and J. K. Rose. 1992. Sorting of GPI-anchored proteins to glycolipid-enriched membrane subdomains during transport to the apical cell surface. *Cell.* **68:** 533–544.
15. Parton, R. G., and K. Simons. 1995. Digging into caveolae. *Science.* **269:** 1398–1399.
16. Harder, T., P. Scheiffele, P. Verkade, and K. Simons. 1998. Lipid domain structure of the plasma membrane revealed by patching of membrane components. *J. Cell Biol.* **141:** 929–942.
17. Anderson, R. G. 1998. The caveolae membrane system. *Annu. Rev. Biochem.* **67:** 199–225.
18. Merrill, A. H., and D. D. Jones. 1990. An update of the enzymology and regulation of sphingomyelin metabolism. *Biochim. Biophys. Acta.* **1044:** 1–12.
19. Futerman, A. H., B. Stieger, A. L. Hubbard, and R. E. Pagano. 1990. Sphingomyelin synthesis in rat liver occurs predominantly at the cis and medial cisternae of the Golgi apparatus. *J. Biol. Chem.* **265:** 8650–8657.
20. Jeckel, D., A. Karrenbauer, R. Birk, R. R. Schmidt, and F. Wieland. 1990. Sphingomyelin is synthesized in the cis Golgi. *FEBS Lett.* **261:** 155–157.
21. Schweizer, A., H. Clausen, G. van Meer, and H. P. Hauri. 1994. Localization of O-glycan initiation, sphingomyelin synthesis, and glucosylceramide synthesis in Vero cells with respect to the endoplasmic reticulum-Golgi intermediate compartment. *J. Biol. Chem.* **269:** 4035–4041.
22. van Helvoort, A., W. van't Hof, T. Ritsema, A. Sandra, and G. van Meer. 1994. Conversion of diacylglycerol to phosphatidylcholine on the basolateral surface of epithelial (Madin-Darby canine kidney) cells. Evidence for the reverse action of a sphingomyelin synthase. *J. Biol. Chem.* **269:** 1763–1769.
23. Moreau, P., and C. Cassagne. 1994. Phospholipid trafficking and membrane biogenesis. *Biochim. Biophys. Acta.* **1197:** 257–290.
24. Obradors, M. J., D. Sillence, S. Howitt, and D. Allan. 1997. The subcellular sites of sphingomyelin synthesis in BHK cells. *Biochim. Biophys. Acta.* **1359:** 1–12.
25. Albi, E., and M. V. Magni. 1999. Sphingomyelin synthase in rat liver nuclear membrane and chromatin. *FEBS Lett.* **460:** 369–372.
26. Albi, E., and M. V. Magni. 2003. Chromatin-associated sphingomyelin: metabolism in relation to cell function. *Cell Biochem. Funct.* **21:** 211–215.
27. Albi, E., S. Pieroni, M. V. Magni, and C. Sartori. 2003. Chromatin sphingomyelin changes in cell proliferation and/or apoptosis induced by ciprofibrate. *J. Cell. Physiol.* **196:** 354–361.
28. Huitema, K., J. Van Den Dikkenberg, J. F. Brouwers, and J. C. Holthuis. 2004. Identification of a family of animal sphingomyelin synthases. *EMBO J.* **23:** 33–44.
29. Yamaoka, S., M. Miyaji, T. Kitano, H. Umehara, and T. Okazaki. 2004. Expression cloning of a human cDNA restoring sphingomyelin synthesis and cell growth in sphingomyelin synthase-defective lymphoid cells. *J. Biol. Chem.* **279:** 18688–18693.
30. Carlson, C. A., D. S. Steinwaerder, H. Stecher, D. M. Shayakhmetov, and A. Lieber. 2002. Rearrangements in adenoviral genomes mediated by inverted repeats. *Methods Enzymol.* **346:** 277–292.
31. Ye, X., M. Liang, X. Meng, X. Ren, H. Chen, Z. Y. Li, S. Ni, A. Lieber, and F. Hu. 2003. Insulation from viral transcriptional regulatory elements enables improvement to hepatoma-specific gene expression from adenovirus vectors. *Biochem. Biophys. Res. Commun.* **307:** 759–764.
32. Hojjati, M. R., and X. C. Jiang. 2006. Rapid, specific, and sensitive measurements of plasma sphingomyelin and phosphatidylcholine. *J. Lipid Res.* **47:** 673–676.
33. Hojjati, M. R., Z. Li, and X. C. Jiang. 2005. Serine palmitoyl-CoA transferase (SPT) deficiency and sphingolipid levels in mice. *Biochim. Biophys. Acta.* **1737:** 44–51.
34. Carr, T. P., C. J. Andresen, and L. L. Rudel. 1993. Enzymatic determination of triglyceride, free cholesterol, and total cholesterol in tissue lipid extracts. *Clin. Biochem.* **26:** 39–42.
35. Jiang, X. C., L. Mucci-Magoulas, J. Mar, M. Lin, A. Walsh, J. L. Breslow, and A. Tall. 1993. Down-regulation of mRNA for the low density lipoprotein receptor in transgenic mice containing the gene for human cholesteryl ester transfer protein. Mechanism to

explain accumulation of lipoprotein B particles. *J. Biol. Chem.* **268:** 27406–27412.
36. Meng, A., C. Luberto, P. Meier, A. Bai, X. Yang, Y. A. Hannun, and D. Zhou. 2004. Sphingomyelin synthase as a potential target for D609-induced apoptosis in U937 human monocytic leukemia cells. *Exp. Cell Res.* **292:** 385–392.
37. Matthews, C. M. E. 1957. The theory of tracer experiments with ^{131}I-labeled plasma proteins. *Phys. Med. Biol.* **2:** 36–53.
38. Schissel, S. L., X. C. Jiang, J. Tweedie-Hardman, T. S. Jeong, E. H. Camejo, J. Najib, J. H. Rapp, K. J. Williams, and I. Tabas. 1998. Secretory sphingomyelinase, a product of the acid sphingomyelinase gene, can hydrolyze atherogenic lipoproteins at neutral pH. *J. Biol. Chem.* **273:** 2738–2746.
39. Wong, M. L., B. Xie, N. Beatini, P. Phu, S. Marathe, A. Johns, P. W. Gold, E. Hirsch, K. J. Williams, J. Licinio, et al. 2000. Acute systemic inflammation up-regulates secretory sphingomyelinase in vivo: a possible link between inflammatory cytokines and atherogenesis. *Proc. Natl. Acad. Sci. USA.* **97:** 8681–8686.
40. Acton, S., A. Rigotti, K. T. Landschultz, S. Xu, H. H. Hobbs, and M. Krieger. 1996. Identification of scavenger receptor SR-BI as a high density lipoprotein receptor. *Science.* **271:** 518–520.
41. Mardones, P., V. Quinones, L. Amigo, M. Moreno, J. F. Miquel, M. Schwarz, H. E. Miettinen, B. Trigatti, M. Krieger, S. Van Patten, et al. 2001. Hepatic cholesterol and bile acid metabolism and intestinal cholesterol absorption in scavenger receptor class B type I-deficient mice. *J. Lipid Res.* **42:** 170–180.
42. Lee, J. Y., and J. S. Parks. 2005. ATP-binding cassette transporter AI and its role in HDL formation. *Curr. Opin. Lipidol.* **16:** 19–25.
43. Ridgway, N. D. 1995. 25-Hydroxycholesterol stimulates sphingomyelin synthesis in Chinese hamster ovary cells. *J. Lipid Res.* **36:** 1345–1358.
44. Lagace, T. A., D. M. Byers, H. W. Cook, and N. D. Ridgway. 1999. Chinese hamster ovary cells overexpressing the oxysterol binding protein (OSBP) display enhanced synthesis of sphingomyelin in response to 25-hydroxycholesterol. *J. Lipid Res.* **40:** 109–116.
45. Miro-Obradors, M. J., J. Osada, H. Aylagas, I. Sanchez-Vegazo, and E. Palacios-Alaiz. 1993. Microsomal sphingomyelin accumulation in thioacetamide-injured regenerating rat liver: involvement of sphingomyelin synthase activity. *Carcinogenesis.* **14:** 941–946.
46. Luberto, C., and Y. A. Hannun. 1998. Sphingomyelin synthase, a potential regulator of intracellular levels of ceramide and diacylglycerol during SV40 transformation. Does sphingomyelin synthase account for the putative phosphatidylcholine-specific phospholipase C? *J. Biol. Chem.* **273:** 14550–14559.
47. van den Hill, A., G. P. van Heusden, and K. W. Wirtz. 1985. The synthesis of sphingomyelin in the Morris hepatomas 7777 and 5123D is restricted to the plasma membrane. *Biochim. Biophys. Acta.* **833:** 354–357.
48. Bourteele, S., A. Hausser, H. Doppler, J. Horn-Muller, C. Ropke, G. Schwarzmann, K. Pfizenmaier, and G. Muller. 1998. Tumor necrosis factor induces ceramide oscillations and negatively controls sphingolipid synthases by caspases in apoptotic Kym-1 cells. *J. Biol. Chem.* **273:** 31245–31251.
49. Miller, N. E., and G. J. Miller. 1975. High-density lipoprotein and atherosclerosis [letter]. *Lancet.* **1:** 1033.
50. Williams, K. J., and I. Tabas. 1995. The response-to-retention hypothesis of early atherosclerosis. *Arterioscler. Thromb. Vasc. Biol.* **15:** 551–561.
51. Rhainds, D., P. Bourgeois, G. Bourret, K. Huard, L. Falstrault, and L. Brissette. 2004. Localization and regulation of SR-BI in membrane rafts of HepG2 cells. *J. Cell Sci.* **117:** 3095–3105.
52. Burgos, P. V., C. Klattenhoff, E. de la Fuente, A. Rigotti, and A. Gonzalez. 2004. Cholesterol depletion induces PKA-mediated basolateral-to-apical transcytosis of the scavenger receptor class B type I in MDCK cells. *Proc. Natl. Acad. Sci. USA.* **101:** 3845–3850.
53. Peng, Y., W. Akmentin, M. A. Connelly, S. Lund-Katz, M. C. Phillips, and D. L. Williams. 2004. Scavenger receptor BI (SR-BI) clustered on microvillar extensions suggests that this plasma membrane domain is a way station for cholesterol trafficking between cells and high-density lipoprotein. *Mol. Biol. Cell.* **15:** 384–396.
54. Mendez, A. J., G. Lin, D. P. Wade, R. M. Lawn, and J. F. Oram. 2001. Membrane lipid domains distinct from cholesterol/sphingomyelin-rich rafts are involved in the ABCA1-mediated lipid secretory pathway. *J. Biol. Chem.* **276:** 3158–3166.
55. Hannun, Y. A., and C. Luberto. 2000. Ceramide in the eukaryotic stress response. *Trends Cell Biol.* **10:** 73–80.
56. Kolesnick, R. 2002. The therapeutic potential of modulating the ceramide/sphingomyelin pathway. *J. Clin. Invest.* **110:** 3–8.
57. Jaffrezou, J. P., G. Laurent, and T. Levade. 2002. Ceramide in regulation of apoptosis. Implication in multitoxicant resistance. *Subcell. Biochem.* **36:** 269–284.
58. Goni, F. M., and A. Alonso. 1999. Structure and functional properties of diacylglycerols in membranes. *Prog. Lipid Res.* **38:** 1–48.
59. Schlitt, A., S. Blankenberg, D. Yan, H. von Gizycki, M. Buerke, K. Werdan, C. Bickel, K. J. Lackner, J. Meyer, H. J. Rupprecht, et al. 2006. Further evaluation of plasma sphingomyelin levels as a risk factor for coronary artery disease. *Nutr. Metab. (Lond).* **3:** 5–10.